Experimental and Theoretical Multiple Kinetic Isotope Effects for an S_N2 Reaction. An Attempt to Determine Transition-State Structure and the Ability of Theoretical Methods to Predict Experimental Kinetic Isotope Effects

Yao-ren Fang,[a] Ying Gao,[a] Per Ryberg,[c] Jonas Eriksson,[c] Magdalena Kołodziejska-Huben,[b] Agnieszka Dybała-Defratyka,[b] S. Madhavan,[d] Rolf Danielsson,[e] Piotr Paneth,*[b] Olle Matsson,*[c] and Kenneth Charles Westaway*[a]

Abstract: The secondary α-deuterium, the secondary β-deuterium, the chlorine leaving-group, the nucleophile secondary nitrogen, the nucleophile $^{12}C/^{13}C$ carbon, and the $^{11}C/^{14}C$ α-carbon kinetic isotope effects (KIEs) and activation parameters have been measured for the S_N2 reaction between tetrabutylammonium cyanide and ethyl chloride in DMSO at 30 °C. Then, thirty-nine readily available different theoretical methods, both including and excluding solvent, were used to calculate the structure of the transition state, the activation energy, and the kinetic isotope effects for the reaction. A comparison of the experimental and theoretical results by using semiempirical, ab initio, and density functional theory methods has shown that the density functional methods are most successful in calculating the experimental isotope effects. With two exceptions, including solvent in the calculation does not improve the fit with the experimental KIEs. Finally, none of the transition states and force constants obtained from the theoretical methods was able to predict all six of the KIEs found by experiment. Moreover, none of the calculated transition structures, which are all early and loose, agree with the late (product-like) transition-state structure suggested by interpreting the experimental KIEs.

Keywords: ab initio calculations · density functional calculations · isotope effects · nucleophilic substitution · semiempirical calculations · transition states

[a] Prof. K. C. Westaway, Y.-r. Fang, Dr. Y. Gao
Department of Chemistry and Biochemistry, Laurentian University
Sudbury, Ontario P3E 2C6 (Canada)
Fax: (+1) 705-675-4844
E-mail: kwestaway@laurentian.ca

[b] Prof. P. Paneth, Dr. M. Kołodziejska-Huben, Dr. A. Dybała-Defratyka
Institute of Applied Radiation Chemistry
Technical University of Łodz
Wroblewskiego 15, 90-924 Łodz (Poland)
Fax: (+48) 42-636-5008
E-mail: paneth@p.lodz.pl

[c] Prof. O. Matsson, Dr. P. Ryberg, J. Eriksson
Department of Organic Chemistry, Institute of Chemistry
Uppsala University, P.O. Box 599, 75124 Uppsala (Sweden)
Fax: (+46) 18-471-3818
E-mail: ollem@kemi.uu.se

[d] S. Madhavan
Department of Biochemistry, University of Nebraska
Lincoln, Nebraska, 68588-0664 (USA)

[e] Dr. R. Danielsson
Department of Analytical Chemistry, Institute of Chemistry
Uppsala University, P.O. Box 599, 75124 Uppsala (Sweden)

Introduction

Chemists have been trying to determine the structure of the transition states of organic reactions for several decades.[1–5] The initial approach was to use kinetic isotope effects (KIEs) to estimate the relative amount of bond formation or bond rupture in the transition state of a reaction. However, most of the early studies determined only one KIE in a reaction.[6] For instance, workers would determine only the chlorine leaving-group KIE in an S_N2 reaction of an alkyl chloride, Equation (1).

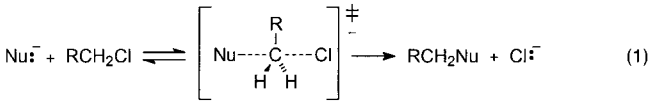

(1)

While the chlorine isotope effect gave some information about the α-carbon–leaving-group bond in the S_N2 transition state, it did not characterize the whole transition state.

The initial problem of measuring only one isotope effect for a reaction has been overcome by measuring several isotope

© 2003 Wiley-VCH Verlag GmbH & Co. KGaA, Weinheim
DOI: 10.1002/chem.200204119

effects in a reaction, and recently the structure of several S_N2 transition states have been elucidated in considerable detail.[4, 7–9] However, other problems have been encountered even when more KIEs are determined for a reaction. For instance, it is necessary to consider the coupling between different vibrations in the transition state when interpreting certain KIEs.[10] Another problem is that some KIEs, for example, secondary α-deuterium (2° α-D)[11, 12] and α-carbon KIEs, are difficult to interpret because they depend on the bonding of the isotopic atom to two or more atoms in the ground and in the transition state.[13, 14]

Another approach to determining transition structure has been to use theoretical methods. The initial methods such as the BEBOVIB calculations, which used experimental KIEs to suggest transition structure,[13, 15, 16] were crude, partly because they were based on equations that represented the change in energy with structure for bonds close to their ground-state configuration in order to determine the geometry of a transition structure that was far from the ground-state configuration. A second problem with early quantum-chemical approaches was that they only applied to the gas phase and not to solution for which the experimental kinetic isotope effects were measured and where the reaction takes place.[7, 18] This uncertainty, due to the lack of solvation in the theoretical approach, was demonstrated when research indicated that the solvation energy for simple organic reactions was large and that the free energies of activation including solvent were very different from those calculated in the gas phase. This solvation problem was also demonstrated by the work of Bohme and co-workers[19] and others[20, 21] who showed that the reaction coordinate was different for S_N2 reactions in the gas phase and in solution. Another problem that plagued the theoretical approach to determining transition-state structure was that only the largest computers were able to calculate the structure of even medium-sized molecules accurately.

However, the recent advances in theoretical methods, coupled with the enormous increase in the power of computers, have enabled chemists to calculate transition structures for larger molecules. These developments suggest that the gap between theory and experiment should be narrowing. This study, which compares the transition structure and the kinetic isotope effects obtained from various computational methods with the experimental kinetic isotope effects for a simple S_N2 reaction, has been undertaken in an effort to determine the ability of theory to calculate kinetic isotope effects from a calculated transition structure and the corresponding force constants.

The reaction chosen for this investigation was the S_N2 reaction between ethyl chloride and tetrabutylammonium cyanide in DMSO at $30\,^\circ$C, Equation (2).

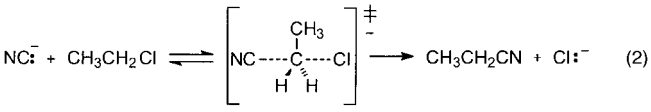

(2)

This reaction was chosen for two reasons. First, the molecules are small enough to enable a high level of theory to be applied to the reaction. This means that one has the ability to obtain unbiased geometries and force constants for the reactants and transition structure that allow the kinetic isotope effects to be calculated. The second reason for choosing this reaction is that a kinetic isotope effect could be determined for all but one of the atoms in the S_N2 transition state. In particular, the chlorine leaving group, the 2° α-D_2, the 2° β-D_3, the primary nucleophile carbon, the secondary nucleophile nitrogen, and the α-carbon kinetic isotope effects have been measured for this simple S_N2 reaction. These KIEs allow a detailed structure for the transition state to be suggested. This study is important because it provides a complete set of experimental data that can be used to do a very detailed and thorough test of the ability of various levels of theory to calculate the transition-state structure and the kinetic isotope effects for a reaction.

Results and Discussion

The 2° α-D_2 KIE: The 2° α-D_2 KIE for the ethyl chloride–cyanide ion S_N2 reaction, see Table 1, was $k_H/k_D = 0.990 \pm 0.004$.

Table 1. The second-order rate constants and 2° α-D_2 kinetic isotope effect for the S_N2 reaction between tetrabutylammonium cyanide and ethyl chloride in DMSO at $30.000\,^\circ$C.

Experiment	$10^4 k_H$ [$M^{-1}s^{-1}$]	$10^4 k_D$ [$M^{-1}s^{-1}$]	$(k_H/k_D)_{\alpha\text{-}D2}$
1	4.169	4.231	0.9854
2	4.346	4.381	0.9920
3	4.168	4.219	0.9879
4	4.244	4.266	0.9948
Average			0.990 ± 0.004[a]

[a] Standard deviation.

The 2° α-D_2 KIE was determined by dividing the rate constants measured separately for the isotopomers. The slightly inverse value indicates that the C_α–H(D)[23] vibrations are approximately the same in the reactants and the transition state.[22, 24] This suggests that the transition state is at least as sterically crowded as the reactant and that the transition state is reasonably tight with either a short α-carbon–chlorine (C_α–Cl) and/or a short cyanide-carbon–carbon (NC–C_α) bond.[11, 12] Another indication that the transition state is crowded (tight) is that the 2° α-D_2 KIE for the S_N2 reaction between *n*-butyl chloride and the thiophenoxide ion in DMSO is 1.125 ± 0.008, that is, much larger than the 2° α-D KIE in this reaction.[25] Since the magnitude of the 2° α-D KIE is determined mainly by the nucleophile–leaving group separation in the S_N2 transition state[11] and since both the ethyl and butyl substrates are primary substrates and the reaction (S_N2) and the solvent are the same, the ethyl chloride transition state must be much tighter with a shorter nucleophile–leaving group separation than the butyl chloride reaction. Thus, the magnitude of the KIE also suggests that the ethyl chloride transition state is tight. If the transition state is reasonably symmetric, then both the NC–C_α and the C_α–Cl bond lengths must be short. A second possibility is that the transition state is asymmetric and that either the NC–C_α or the C_α–Cl bond is short and the other reacting bond long.[12] In

 © 2003 Wiley-VCH Verlag GmbH & Co. KGaA, Weinheim

fact, a transition state with a short NC–C_α bond and a long C_α–Cl bond seems the most likely because:

i) Matsson et al.[8] concluded on the basis of small nucleophile carbon KIEs ranging from 1.0105 to 1.0070, small and constant[12] 2° α-D_2 KIEs ranging from 1.011 to 1.002,[26] and large and variable chlorine leaving-group KIEs of between 1.0060 and 1.0079,[27] that the transition state for the S_N2 reaction between *p*-substituted benzyl chlorides and the cyanide ion had a short NC–C_α and a long C_α–Cl bond.

ii) KIE data measured for several S_N2 reactions have suggested that the stronger reacting bond is short and that the weaker reacting bond is long in an S_N2 transition state.[8, 9, 12, 28] In the cyanide ion – ethyl chloride reaction, the new NC–C_α bond is much stronger than the C_α–Cl bond.

Therefore, one would infer that the NC–C_α bond would be short and the C_α–Cl bond would be long in the transition state.

The 2° β-D_3 KIE: The 2° β-D_3 KIE was determined by dividing the rate constants measured separately for the isotopomers.

The 2° β-D_3 KIE of $k_H/k_D = 1.014 \pm 0.003$, see Table 2, is small and normal. This is typical of the 2° β-D KIEs reported for other S_N2 reactions.[29, 30] However, the small value indicates that there is very little positive charge on the α-carbon in the transition state of this reaction, that is, the hyperconjugative contribution to the isotope effect, which becomes significant as the positive charge on the α-carbon increases, will be effectively zero and a small normal inductive and/or steric 2° β-D KIE is observed.[30] This small 2° β-D KIE is consistent with the small 2° α-D KIE; this suggests that at least one of the reacting bonds in the transition state is short, that is, that there is little or no positive charge, and perhaps even a small negative charge on the α-carbon in the transition state. Inductive and steric secondary β-deuterium KIEs for S_N2 reactions are usually small and inverse.[22, 24] A normal inductive 2° β-D KIE could be observed if the transition state were tight, that is, had increased total bonding and a slight negative charge on the α-carbon.

Table 2. The second order rate constants and the 2° β-D_3 kinetic isotope effect for the S_N2 reaction between tetrabutylammonium cyanide and ethyl chloride in DMSO at 30.000 °C.

Experiment	$10^4 k_H$ [$M^{-1}s^{-1}$]	$10^4 k_D$ [$M^{-1}s^{-1}$]	$(k_H k_D)_{\beta\text{-}D3}$
1	4.310	4.237	1.017
2	4.392	4.337	1.013
3	4.388	4.339	1.011
Average			1.014 ± 0.003[a]

[a] Standard deviation.

The chlorine leaving-group KIE: A normal chlorine leaving-group KIE of $k^{35}/k^{37} = 1.0070 \pm 0.0003$, see Table 3, was found for the ethyl chloride – cyanide ion S_N2 reaction. The chlorine KIE was determined by isotope-ratio mass spectrometry.

This large KIE, which is approximately 50% of the theoretical maximum chlorine leaving-group KIE of 1.014,[31, 32] indicates that there is significant C_α–Cl bond rupture in the transition state. This KIE is as large as those found in several other S_N2 reactions of alkyl chlorides in which the C_α–Cl transition-state bond is thought to be quite long.[8, 27, 28] For instance, the chlorine KIE for this reaction is as large as many of the chlorine leaving-group KIEs found for benzyl substrates that are thought to have much looser transition states than ethyl substrates.

Table 3. The chlorine leaving-group KIEs for the S_N2 reaction between tetrabutylammonium cyanide and ethyl chloride in DMSO at 30.00 °C.

Sample	δ value[a]	Average fraction of reaction (*f*)	R_o/R_f[b]	k^{35}/k^{37}
1	– 7.33	0.158	0.993784	1.00683
2	– 7.54	0.179	0.993576	1.00715
3	– 7.00	0.217	0.994109	1.00672
4	– 7.49	0.249	0.993626	1.00743
5	– 7.25	0.187	0.993862	1.00686
6	– 7.18	0.279	0.993932	1.00722
7	– 7.15	0.248	0.993961	1.00703
8	– 6.75	0.276	0.994356	1.00670
Average				1.00699 ± 0.00026[c]

[a] The δ-value is the difference between the $^{35}Cl/^{37}Cl$ ratio in the methyl chloride sample obtained from the experiment and the $^{35}Cl/^{37}Cl$ ratio in a standard methyl chloride sample, in ppm. [b] R_f = ratio of $^{35}Cl/^{37}Cl$ in the chloride ion at *f*. R_o = ratio of $^{35}Cl/^{37}Cl$ in the chloride ion at 100% completion. [c] Standard deviation.

The α-carbon KIE: The α-carbon KIE of $k^{11}/k^{14} = 1.21 \pm 0.02$, see Table 4, for the ethyl chloride – cyanide ion S_N2 reaction is large and normal. It was determined by direct determination of the isotopic ratios by using an HPLC/liquid scintillation technique.

Lynn and Yankwich[33] reported an α-^{13}C KIE of 1.0711 ± 0.0078 for the S_N2 reaction of the cyanide ion with methyl chloride in water at 31 °C. Their value corresponds to $k^{11}/k^{14} = 1.22 - 1.23$,[13, 34, 35] which is within the experimental error of the value found for our ethyl chloride – cyanide ion reaction in DMSO. These KIEs are large and close to the maximum α-carbon KIE. A near-maximum α-carbon KIE, $k^{12}/k^{13} = 1.0713 \pm 0.0046$,[36] was also found for the reaction of the

Table 4. The α-carbon kinetic isotope effect for the S_N2 reaction between tetrabutylammonium cyanide and ethyl chloride in DMSO at 30.00 °C.

Experiment	Sample[a]	Fraction of reaction (*f*)	R_f/R_0[b]	k^{11}/k^{14}	Average for each experiment
1	1	0.52	1.13944	1.2181	
	2	0.67	1.22413	1.2227	
	3	0.77	1.28696	1.2090	1.2166
2	1	0.31	1.05159	1.1598	
	2	0.54	1.14250	1.2066	
	3	0.67	1.20611	1.2014	
	4	0.77	1.26752	1.1897	1.1894
3	1	0.75	1.29821	1.2292	
	2	0.83	1.39594	1.2334	1.2313
4	1	0.47	1.11920	1.2138	
	2	0.63	1.18403	1.2045	
	3	0.73	1.25048	1.2097	1.2093
Total average					1.208 ± 0.019[c]

[a] In each experiment samples of cyanide ion were collected at various fractions of reaction, *f*. [b] R_f = ratio of $^{14}C/^{11}C$ in the reactant ethyl chloride at fraction of reaction *f*. R_0 = ratio of $^{14}C/^{11}C$ in the reactant ethyl chloride at the start of the reaction ($t = 0$). [c] Standard deviation.

© 2003 Wiley-VCH Verlag GmbH & Co. KGaA, Weinheim

cyanide ion with methyl iodide; an even larger $k^{12}/k^{13} = 1.0815 \pm 0.0068$[33] was found for the methyl bromide–cyanide ion reaction in water at 31 °C. The α-$^{11}C/^{14}C$ KIEs for Menshutkin reactions of methyl iodide with various amines range from 1.189 ± 0.012 (2,4-lutidine in acetonitrile) to 1.221 ± 0.006 (triethylamine in dimethoxyethane),[37, 38] and reaction with the hydroxide ion in 50 % dioxane/water yielded a value of 1.192 ± 0.001.[13] Thus, all these α-carbon KIEs are large, the smallest being about 85 % of the largest-observed KIE. The qualitative conclusion would be that all these S_N2 reactions have rather symmetric transition states, since the maximum α-carbon KIE is expected for a symmetric transition state. However, the interpretation will be dependent on the shape of the dependence of the KIE on the position of the transition state along the reaction coordinate. A curve with a narrow maximum means that the α-carbon KIE is very sensitive to transition-state structure, whereas a broader curve implies that the KIE is not very sensitive to a change in transition-state structure.

Matsson and co-workers reported BEBOVIB calculations of the α-$^{11}C/^{14}C$ KIEs for the S_N2 reactions of methyl iodide and either the hydroxide ion[13] or *N,N*-dimethyltoluidine.[37] Their calculations showed that the choice of reaction-coordinate model strongly affected the dependence of the KIE on the bond order of the breaking and forming bonds, that is, depending on whether or not the interaction force constants were allowed to vary with transition-state geometry, a narrow or broad curve described the dependence of the KIE on the total bond order. However, application of a reaction-coordinate model in which the methyl hydrogen bending vibrations were coupled by interaction force constants to the stretching vibrations for the nucleophile–α-carbon and C_α–I bonds,[39] was necessary to reproduce the large experimental KIEs. For instance, in the methyl iodide–hydroxide ion reaction, a bond order (the sum of the O–C_α and the C_α–I bond orders was 1.00) for the forming O–C_α bond ranging from 0.30 to 0.55 when the interaction force constants were allowed to vary, or from 0.15 to 0.65 when the interaction force constants were fixed gave a KIE that was ≥ 77 % of the maximum value of 1.22.[13] This curve with a broad maximum describing the dependence of the KIE on transition-state structure suggests that large α-carbon KIEs would be observed for transition states that are early, symmetric, or late. This idea is supported by the observation that the α-carbon KIEs for several S_N2 reactions with different nucleophiles and leaving groups, which must have different transition-state structures, are all near the maximum value. Therefore, the experimentally determined value of 1.21 for the ethyl chloride–cyanide ion reaction could be consistent with either an early, a late, or a symmetric transition state. Unfortunately, until the dependence of these KIEs on transition-state structure is known with certainty, α-carbon KIEs will only be useful for indicating the mechanism of the reaction but will not be particularly useful for determining transition-state structure unless there is a systematic change in a KIE within a series of reactions.

The nucleophile 2° nitrogen KIE: The very small (null) nucleophile 2° N KIE of $k^{14}/k^{15} = 1.0002 \pm 0.0006$, see Table 5, indicates, as expected, that there is little or no change in bonding to the cyanide ion nitrogen atom on going from reactants to the transition state.

Table 5. The isotopic composition and the nucleophile 2° nitrogen and nucleophile carbon KIEs for the S_N2 reaction between tetrabutylammonium cyanide and ethyl chloride in DMSO at 30.0 °C.

Sample	Fraction of reaction (f)	δ-^{13}C[a]	δ-^{15}N[b]
1	0.68	– 1.389	– 40.65
2	0.52	– 0.857	– 39.495
3	0.45	– 0.823	– 39.572
4	0.38	– 0.766	– 38.571
5	0.28	– 0.91	– 40.419
6	0.22	– 1.054	– 41.065
7	0.61	– 1.148	– 40.64
8	0.46	– 1.477	– 41.676
9	0.42	– 1.342	– 39.828
10	0.37	– 1.187	– 41.364
11	0.2	– 2.04	– 40.737
12	0.74	– 1.354	– 39.364
13	0.56	– 0.889	– 38.49
14	0.51	– 1.552	– 39.35
15	0.37	– 0.909	–
16	0.3	– 1.769	–
18	0.23	– 1.652	–
Average isotope effect		1.0009 ± 0.0007[c]	1.0002 ± 0.0006[c]

[a] $\delta^{13}C$ relative to PDB standard. [b] $\delta^{15}N$ relative to home standard nitrogen gas. [c] Standard deviation.

The nucleophile carbon KIE: The nucleophile carbon KIE was determined to be $k^{12}/k^{13} = 1.0009 \pm 0.0007$, see Table 5.

A nucleophile KIE is best understood in terms of Equation (3):

$$k_L/k_H = (\nu_L^{\ddagger}/\nu_H^{\ddagger})[1 - \Sigma G(u_i^{\ddagger})\Delta u_i^{\ddagger} + \Sigma G(u_i)\Delta u_i] \quad (3)$$

in which $G(u_i) = [\frac{1}{2} - 1/u_i + 1/(e^{u}i - 1)]$ and $\Delta u_i = hc/kT(\Delta\omega_i)$. The terms h, c, k, and T are Planck's constant, the speed of light, Boltzmann's constant and the absolute temperature, respectively. $\Delta\omega_i$ is the change in frequency of a vibration (expressed in cm^{-1}) caused by the isotopic substitution. This means a smaller normal or more inverse KIE is observed when there is more NC–C_α bond formation in the transition state.

The nucleophile KIE is made up of a normal temperature-independent factor ($\nu_L^{\ddagger}/\nu_H^{\ddagger}$, estimated as 1.02[8]) and an inverse temperature-dependent factor $(1 - \Sigma G(u_i^{\ddagger})\Delta u_i^{\ddagger} + \Sigma G(u_i)\Delta u_i)$ that is related to the additional bonding that occurs between the nucleophile and the α-carbon in the transition state. Thus the zero-point energy for the vibrational modes involving motion of the nucleophilic carbon is greater in the transition state than in the reactant.

Based on the small and constant 2° α-D KIEs[12, 26] and the large and variable chlorine KIEs,[27] (vide supra) Matsson et al.[8] interpreted the nucleophile $^{11}C/^{14}C$ KIEs of 1.0070–1.0105 observed for the S_N2 reactions between several *para*-substituted benzyl chlorides and the cyanide ion (a temperature-dependent factor of approximately 0.99) as having a short NC–C_α carbon bond in the transition state. The

 © 2003 Wiley-VCH Verlag GmbH & Co. KGaA, Weinheim

observed k^{12}/k^{13} of 1.0009 would be equivalent to a k^{11}/k^{14} of 1.0027, (a temperature-dependent factor of approximately 0.98 for the observed KIE). Therefore the NC–C_α bond in the ethyl chloride – cyanide ion S_N2 transition state must be shorter (the smaller KIE indicates there is more NC–C_α bonding in the transition state) than in the benzyl chloride – cyanide ion transition state. The incoming carbon KIE is difficult to interpret because one does not know how close the nucleophile has to come to the α-carbon to raise the zero-point energy and thereby to reduce the magnitude of the KIE.[41] However, based on previous work, the NC–C_α bond is thought to be short in the transition state.

The transition-state structure based on experimental KIEs: The large chlorine leaving-group KIE ($k^{35}/k^{37} = 1.0070 \pm 0.00007$) suggests there is considerable C_α–Cl bond rupture in the transition state. The small inverse 2° α-D_2 KIE of 0.990 ± 0.004 on the other hand suggests that the transition structure is either symmetric and tight with short NC–C_α and C_α–Cl bonds or asymmetric with either a short NC–C_α or a short C_α–Cl bond. The large chlorine KIE is only consistent with an asymmetric transition state with a short NC–C_α and a long C_α–Cl bond. This interpretation is supported by the small 2° β-D_3 KIE of 1.014 ± 0.003, because there would be very little positive charge on C_α in the asymmetric transition state suggested by the chlorine and 2° α-D_2 KIEs. This interpretation is also supported by the small nucleophile carbon KIE of 1.0009 ± 0.0007 found for the ethyl chloride – cyanide ion S_N2 reaction. Therefore, the best interpretation of the KIE data is that the S_N2 transition state is asymmetric with a short NC–C_α and a long C_α–Cl bond.

Finally, it is interesting to compare the transition-state structure suggested by the KIEs measured in this study with the transition-state structure suggested by Matsson et al. for the similar S_N2 reaction between benzyl chloride and the cyanide ion in DMSO at 30 °C.[8] The chlorine KIEs for these two reactions are almost identical, that is, a slightly larger $k^{35}/k^{37} = 1.0072$ was found for the benzyl chloride reaction. A $k^{35}/k^{37} = 1.0070$ was found for the ethyl chloride reaction. This suggests that C_α–Cl-bond rupture is very slightly larger in the benzyl chloride transition state. However, the smaller (more inverse) 2° α-D (0.990 versus 1.011) and the small 2° β-D KIEs found for the ethyl chloride reaction suggest that the ethyl chloride has a tighter transition state than the benzyl chloride transition state. This suggestion is supported by the smaller nucleophile carbon KIE found for the ethyl chloride reaction. It is interesting that the difference is mainly in the stronger reacting bond, that is, the KIEs suggest the ethyl chloride transition state has a shorter NC–C_α bond and a very slightly shorter (almost identical) C_α–Cl bond compared with the benzyl chloride transition state. It is worth noting that the KIEs suggest that both these cyanide-ion S_N2 reactions in DMSO have similar transition states, that is, both reactions have a short NC–C_α bond and a long C_α–Cl bond.

Activation parameters: The activation parameters, see Table 6, were also measured for the ethyl chloride – cyanide ion reaction. This was done so that the enthalpy of activation could also be used to assess the results from the different theoretical methods in which solvation was included in the calculations. The activation parameters were not calculated for the gas-phase models in which the reaction coordinate[20, 21] and the activation parameters are very different from those in solution.[19]

Table 6. The activation parameters (standard state) for the S_N2 reaction between tetrabutylammonium cyanide and ethyl chloride in DMSO.

T [°C]	$10^4 k$ [$M^{-1}s^{-1}$]	$\Delta G^{\neq}$ [kcal mol^{-1}]	$\Delta H^{\neq}$ [kcal mol^{-1}]	$\Delta S^{\neq}$ [cal K^{-1} mol^{-1}]
25.07	3.952	22.6 ± 0.1	18.7 ± 0.1	-13.2 ± 0.1
35.10	10.73			
40.00	18.04			

The theoretical models: Forty-two different theoretical methods have been used to calculate the structure of the transition state and the experimental KIEs for the ethyl chloride – cyanide ion S_N2 reaction for an S_N2 reaction. The calculations were performed within conventional transition-state theory and neither variational effects nor tunneling were included. Although this approach seems crude at first glance, it is reasonable because variational effects for S_N2 reactions between an ion and a neutral molecule are usually small,[42] and tunneling only has a significant effect on the KIEs of hydrogen. Because the hydrogen atoms of the methyl group are remote from the reaction center, it is safe to assume that the tunneling contribution for these atoms will be negligible. The only improvement upon including tunneling might be for the secondary α-deuterium KIE, but this isotope effect is modeled reasonably well without including tunneling. In most cases, the gas-phase model was used for the reaction that takes place in solution. Evidently, since the gas-phase models cannot be used for predicting the energetics of the reaction, the activation enthalpy was only calculated for the eight methods in which solvation was considered. However, the KIEs of S_N2 reactions in which the nucleophile and the leaving group have the same charge are not affected significantly by a change in the polarity of the solvent.[43–46] Thus, one would expect that including the solvent would have only minimal influence on the results.

Of the forty-two methods used in this study, six were semiempirical calculations that used AM1,[47, 50] PM3,[48] and SAM1[49, 50] Hamiltonians. The 16 ab initio Hartree – Fock (HF) calculations used several basis sets including Truhlar's MIDI!,[51] and ML,[52] Dunning's LANL2DZ,[53] cc-pVDZ,[54] cc-pVTZ,[55] and Pople's 6-31G,[56] and 6-311G.[57, 58] These basis sets were used alone or in combination with diffuse ("aug" in the case of Dunning-style basis sets and "+" for Pople-style basis sets)[59] and polarization functions.[60] The 15 density functional theory (DFT) methods that were used combined standard exchange functionals such as: Becke88,[61] B3,[62] B1,[63] MPW,[64] as well as the nonstandard B(M)[65] exchange functionals with PW91[66] and LYP[67] correlation functionals. Two functionals developed especially for S_N2 reactions, MPW1K[68] and MPW1K-SRP, which is a version of MPW1K that uses specific reaction parameters (SRP),[69] were also used. In these methods, the fraction of Hartree – Fock

© 2003 Wiley-VCH Verlag GmbH & Co. KGaA, Weinheim

exchange has been raised to 60.6% because this apparently gives more accurate potential energy surfaces for this class of reactions. Five post-HF ab initio calculations included were carried out at the MP2,[70] MG3,[71] MC-QCISD,[72] and CASSCF[73] levels. Eight of the methods considered solvent. In the semiempirical calculations, COSMO[74] and SM5.4[75] were used. At the HF and DFT levels, SM5.42,[76] C-PCM-UAHF,[77] PCM-UAHF,[78] and Onsager[79] models were used. All calculations were performed with default convergence criteria and without any constraints on the models of the individual reactants and transition state. A frequency analysis was performed for each stationary point in order to confirm whether this point represented a minimum on the potential-energy surface (no imaginary frequencies) or a first-order saddle point (exactly one imaginary frequency) and to obtain the Hessian matrix necessary for calculating the isotope effects. Calculations that used the SM5.4 model were performed by using Amsol 6.5.1.[80] Calculations that used the COSMO model were performed by using LinMOPAC 2.0.[81] Calculations that involved the multilevel basis set ML were performed by using MULTILEVEL 2.3.[82] All other calculations were performed with Gaussian98.[83] The frequencies used in the KIE calculations were unscaled. The force constants generated in these calculations were transferred to our ISOEFF98 program,[84] and all the KIEs were then calculated.

In all cases, activation enthalpies and KIEs were calculated with respect to isolated reactants. Finally, a comparison of the calculated and experimental KIEs and enthalpy of activation was used to assess the ability of the different theoretical methods to calculate transition-state structure and the experimental isotope effects.

In the absence of any explicit interactions with other molecules, the transition-state structure for the studied reaction should have C_s symmetry, and the Cl-C_α-C_β-$H_{\beta 1}$ torsional angle should be equal to 180° in the optimized structure. The $H_{\beta 1}$ is the hydrogen that is aligned with the incoming cyanide ion in all calculated transition structures. Three methods, the SAM1 calculations in which this torsional angle was equal to 0.6° and two methods that include solvent gave values indicating problems with correct convergence (see below in the Solvent Models section). These three methods were, therefore, not considered in determining the ability of the methods to calculate the KIEs.

Transition structures: Table 7 presents the bond lengths and bond angles for the transition structures of the ethyl chloride–cyanide ion S_N2 reaction calculated by using three semiempirical methods, 16 ab initio methods at the Hartree–Fock (HF) level, five post-HF ab initio methods and 15 DFT methods. There is considerable variation in the transition structures calculated by the 39 different methods. A comparison of the transition structures with reactant and product, ethyl chloride and ethyl nitrile, see Table 7, shows that every theoretical method tested indicates that the transition structure is early and loose. This is because the difference in [(length of the transition structure bond − length of the stable bond in the reactant or product)/length of the normal bond in the reactant or product] × 100% is significantly greater for the cyanide carbon–α-carbon bond than for the α-carbon–chlorine bond, that is, the nucleophile–α-carbon bond is less formed than the α-carbon chlorine bond is broken in all the transition structures regardless of the theoretical method used. For instance, in the DFT transition structures, the NC−C_α bond is between 66 and 55% longer than the NC−C_α bond in the product while the C_α−Cl transition-state bond is between 29 and 18 percent longer than the C_α−Cl in the reactant.

In Table 8, a comparison of the bond lengths and bond angles for the reactants, transition structure, and product are compared at the PCM-UAHF/mPW1PW91/6-31G(d) level of theory. It is worth noting that if one uses Pauling bond orders and the results for the PCM-UAHF/mPW1PW91/6-31G(d) transition structure, rather than the percent extension of the bond in the transition structure, the bond orders were 0.26 and 0.50 for the NC−C_α and C_α−Cl bonds, respectively.[40] This is indeed consistent with an early and loose transition structure.

The theoretically calculated transition structures are evidently not in accord with that based on the experimental interpretation of the six KIEs measured for this reaction. One possibility is that all the theoretical methods fail because they cannot calculate the high-energy transition structure that is far from the ground state correctly and/or because solvation is poorly modeled by the continuum methods. Another explanation is that the conventional framework for interpreting experimental KIEs may be flawed because it is based on empirical generalization and, at least partly, on approximate theory. A third alternative is that neither approach is able to predict the transition structure correctly.

Calculated KIEs: A study by Singleton and co-workers[85] showed that theoretical methods could be used to calculate the transition structure and experimental kinetic isotope effects successfully. However, their study was for a reaction in which neutral reactants were converted into neutral products. This study on the other hand, has tackled a more difficult test for theory, that is, an S_N2 reaction of a negative nucleophile with a neutral reactant to form a charged transition state.

A comparison of the experimental and calculated isotope effects and activation enthalpy by using the different theoretical methods is presented in Table 9 and Figures 1–6, below. At every level of theory, the best results were found for the very small nitrogen KIE. For instance, all but six of the methods predicted this KIE to within the experimental values for this KIE, Figure 1. This was undoubtedly found because there is little or no change in bonding to the cyanide-ion nitrogen on going to the S_N2 transition state. A few (five for the 2° α-D_2 KIE, Figure 2, and fifteen for the chlorine KIE, Figure 3) of the methods gave values that were within the experimental values for these KIEs. The agreement between the other three KIEs, the α-carbon, the nucleophile carbon and the 2° β-D_3 KIEs, Figures 4, 5 and 6, were much poorer. Here, only three, none and none of the calculated KIEs, respectively, fell within the experimental values for these KIEs. Evidently, there are problems with calculating these three kinetic isotope effects by theoretical methods. An analysis of the results for each theoretical method, see

 © 2003 Wiley-VCH Verlag GmbH & Co. KGaA, Weinheim

Table 7. The bond lengths and bond angles found for the transition structures of the ethyl chloride – cyanide ion S_N2 reaction by using the different theoretical methods.

Method	$(N\equiv C)_{TS}$ [Å]	$(NC-C_\alpha)_{TS}$ [Å]	% elongation of $(NC-C_\alpha)$ in TS[a]	$(C_\alpha-Cl)_{TS}$ [Å]	% elongation of $(C_\alpha-Cl)$ in TS[b]	$(C-C_\beta)_{TS}$ [Å]	$(C-H_\alpha)_{TS}$ [Å]	$(C_\beta-H_{\beta1})_{TS}$ [Å]	$(C_\beta-H_\beta)_{TS}$ [Å]	$(NC\text{-}C\text{-}Cl)_{TS}$ [°]
Semiempirical methods										
AM1	1.170	2.086	43.0	2.113	17.1	1.492	1.101	1.118	1.117	164.8
PM3	1.166	2.155	47.7	2.100	16.3	1.494	1.092	1.098	1.097	166.5
COSMO/PM3	1.171	2.238	53.4	2.146	18.9	1.479	1.093	1.100	1.099	164.6
Hartree – Fock methods										
HF/MIDI!	1.147	2.240	53.5	2.357	30.6	1.516	1.060	1.084	1.080	166.8
HF/LANL2DZ	1.176	2.369	62.4	2.363	30.9	1.513	1.062	1.080	1.078	162.7
HF/6-31G(d)	1.153	2.387	63.6	2.305	27.2	1.505	1.061	1.081	1.079	164.6
Onsager/HF/6-31G(d)	1.153	2.333	59.9	2.356	30.5	1.505	1.061	1.081	1.079	162.4
C-PCM-UAHF//HF/6-31G(d)	1.153	2.341	60.5	2.343	27.8	1.503	1.062	1.080	1.079	163.0
PCM-UAHF/HF/6-31G(d)	1.153	2.341	60.5	2.343	29.8	1.503	1.062	1.080	1.079	163.0
SM5.42/HF/6-31G(d)	1.156	2.547	74.6	2.574	42.6	1.482	1.065	1.083	1.080	157.0
HF/6-31 + G(d)	1.155	2.367	62.2	2.363	30.9	1.504	1.062	1.081	1.079	162.6
HF/6-31 + G(d,p)	1.155	2.373	62.6	2.366	31.1	1.503	1.062	1.081	1.079	163.8
HF/6-31 + G(3df,2p)	1.150	2.357	61.5	2.363	30.9	1.504	1.602	1.081	1.080	162.4
HF/6-31 ++ G(d,p)	1.155	2.370	62.4	2.367	31.1	1.503	1.062	1.081	1.080	162.4
HF/6-31 ++ G(3df,2p)	1.150	2.357	61.5	2.363	30.9	1.503	1.062	1.081	1.080	164.0
HF/6-311G(d)	1.147	2.394	64.1	2.339	29.6	1.503	1.061	1.081	1.078	162.5
HF/cc-pVDZ	1.154	2.359	61.7	2.334	29.3	1.505	1.069	1.088	1.086	164.5
HF/aug-cc-pVDZ	1.156	2.370	62.4	2.369	31.2	1.504	1.068	1.086	1.085	163.8
HF/cc-pVTZ	1.145	2.348	61.7	2.357	29.3	1.502	1.059	1.079	1.077	164.1
Post-Hartree – Fock methods										
MP2/6-31G(d)	1.194	2.268	55.4	2.210	22.4	1.511	1.073	1.091	1.088	166.9
CASSCF(4,4)/6-31G(d)	1.176	2.407	65.0	2.291	26.9	1.505	1.061	1.081	1.078	164.3
MP2/6-31 + G(d,p)	1.196	2.236	53.3	2.250	24.7	1.510	1.070	1.088	1.085	166.6
MC-QCISD/ML	1.193	2.266	55.3	2.208	22.3	1.510	1.073	1.091	1.087	167.0
MG3/ML	1.151	2.353	61.3	2.366	31.3	1.500	1.059	1.079	1.077	163.8
DFT methods										
B3LYP/6-31G(d)	1.176	2.392	63.9	2.134	18.2	1.511	1.075	1.094	1.091	164.9
B1LYP/6-31G(d)	1.174	2.387	63.6	2.239	24.0	1.511	1.073	1.093	1.089	164.9
BPW91/6-31G(d)	1.188	2.424	66.1	2.209	22.4	1.515	1.083	1.101	1.098	164.7
MPW1PW91/6-31G(d)	1.174	2.344	60.7	2.198	21.8	1.507	1.075	1.092	1.089	165.8
PCM-UAHF/mPW1PW91/6-31G(d)	1.173	2.265	55.2	2.227	23.4	1.505	1.075	1.091	1.090	164.9
B(M)LYP/6-31G(d)	1.169	2.377	62.9	2.254	24.9	1.509	1.068	1.088	1.085	164.5
MPW1PW91/6-31 + G(d,p)	1.175	2.304	57.9	2.250	24.7	1.505	1.075	1.091	1.089	165.1
MPW1 K/6-31 + G(d,p)	1.166	2.279	56.2	2.240	24.1	1.500	1.069	1.086	1.084	165.6
MPW1 KK-SRP/6-31 + G(d,p)	1.159	2.262	55.0	2.232	23.7	1.495	1.065	1.081	1.079	165.9
B(M)LYP/6-311 ++ G(2d,2p)	1.167	2.331	59.8	2.331	29.1	1.506	1.066	1.085	1.083	164.0
B1LYP/aug-cc-pVDZ	1.175	2.340	60.4	2.296	27.2	1.509	1.077	1.096	1.094	164.21
B3LYP/aug-cc-pVDZ	1.177	2.341	60.5	2.291	26.9	1.509	1.078	1.097	1.095	164.2
C-PCM-UAHF/B3LYP/aug-cc-pVDZ	1.177	2.280	56.3	2.314	28.2	1.506	1.079	1.096	1.095	162.9
PCM-UAHF/B3LYP/aug-cc-pVDZ	1.176	2.285	56.6	2.294	27.1	1.507	1.079	1.096	1.095	162.9
B3LYP/aug-cc-pVTZ	1.165	2.332	59.8	2.295	27.1	1.503	1.070	1.089	1.087	164.1

[a] % $[\{(NC-C_\alpha)_{TS} - (NC-C_\alpha)_{FS}\}/(NC-C_\alpha)_{FS}]$. [b] % $[\{(C_\alpha-Cl)_{TS} - (C_\alpha-Cl)_{IS}\}/(C_\alpha-Cl)_{IS}]$. Here IS = initial state, TS = transition state and FS = final state.

Table 8. The bond lengths and bond angles found for the reactants, transition structure, and product of the ethyl chloride – cyanide ion. S_N2 reaction at the PCM-UAHF/mPW1PW91/6-31G(d) theory level.

	$N\equiv C$ [Å]	$NC-C_\alpha$ [Å]	$C_\alpha-Cl$ [Å]	$C_\alpha-C_\beta$ [Å]	$C_\beta-H_\alpha$ [Å]	$C_\beta-H_{\beta1}$ [Å]	$C_\beta-H_\beta$ [Å]	$NC\text{-}C_\alpha\text{-}Cl$ [°]	$Cl\text{-}C_\alpha\text{-}C_\beta\text{-}H_\beta$ [°]	$Cl\text{-}C_\alpha\text{-}C_\beta\text{-}H_{\beta1}$ [°]
Reactants	1.179	–	1.805	1.509	1.090	1.092	1.095	111.5	119.9	180.0
TS	1.173	2.265	2.227	1.505	1.075	1.091	1.090	164.9	118.7	179.9
Product	1.158	1.459	–	1.529	1.095	1.092	1.092	–	–	–

Table 9, showed that none of the methods predicted the experimental values for all the KIEs.

The agreement between the experimental activation energy of 18.7 ± 0.1 kcal mol^{-1}, Table 9, and the calculated activation enthalpies in the cases in which solvent was considered is excellent for the SM5.42/HF/6-31G(d) and the COSMO/PM3 methods and is reasonable (within 4.5 kcal mol^{-1} of the experimental value) for the PCM-UAHF/6-31G(d), the COSMO/6-31G(d), the PCM-UAHF/mPW1PW91/6-31G(d), and the C-PCM-UAHF and PCM-UAHF/B3LYP/aug-cc-pVDZ models. Unacceptable results for the activation energy were obtained from the Onsager/6-31G(d) (-0.7 kcal mol^{-1}),

© 2003 Wiley-VCH Verlag GmbH & Co. KGaA, Weinheim

Table 9. A comparison of the experimental and theoretical KIEs and activation enthalpies for the S_N2 reaction between ethyl chloride and the cyanide ion in DMSO at 30 °C. The rank based on all the KIEs (excluding the ^{15}N KIE) for each method is given in parenthesis in column 1. The rank for each KIE is given in parenthesis after the theoretical KIE.

Isotope Effect	$(k_H/k_D)_{\alpha\text{-}D2}$	$(k_H/k_D)_{\beta\text{-}D3}$	k^{11}/k^{14}	k^{12}/k^{13}	k^{14}/k^{15}	k^{35}/k^{37}	$\Delta H^{\neq}$ [kcal mol^{-1}]
Experiment	0.990 ± 0.004	1.014 ± 0.003	1.21 ± 0.02	1.0009 ± 0.0007	1.0002 ± 0.0006	1.0070 ± 0.0003	18.7 ± 0.1
Semiempirical methods							
AM1 (21)	0.920 (36)	0.989 (7)	1.20 (1)	0.987 (39)	0.9993 (28)	1.0075 (18)	
PM3 (38)	1.073 (38)	1.045 (10)	1.17 (19)	0.990 (30)	0.9995 (18)	1.0039 (39)	
COSMO/PM3 (34)	1.070 (37)	1.085 (35)	1.17 (19)	0.993 (7)	1.0010 (32)	1.0054 (32)	19.1
Hartree – Fock methods							
HF/MIDI! (39)	0.927 (34)	0.927 (39)	1.18 (14)	0.988 (38)	0.9991 (30)	1.0073 (14)	
HF/LANL2DZ (30)	1.031 (33)	0.953 (19)	1.17 (19)	0.990 (30)	1.0000 (1)	1.0066 (15)	
HF/6-31G(d) (13)	0.978 (13)	0.954 (18)	1.17 (19)	0.9922 (16)	0.9999 (4)	1.0072 (11)	
Onsager/HF/6-31G(d) (23)	0.959 (32)	0.938 (36)	1.19 (4)	0.999 (2)	0.9990 (33)	1.0082 (29)	− 0.7
C-PCM-UAHF/HF/6-31G(d) (37)	0.971 (22)	0.932 (38)	1.19 (4)	0.989 (36)	0.9983 (37)	1.0086 (33)	23.1
PCM-UAHF/HF/6-31G(d) (34)	0.970 (24)	0.933 (37)	1.19 (4)	0.990 (30)	1.0000 (1)	1.0087 (35)	23.2
SM5.42/HF/6-31G(d) (36)	1.127 (39)	1.052 (13)	1.15 (38)	0.996 (3)	1.0012 (35)	1.0092 (38)	18.7
HF/6-31 + G(d) (18)	0.994 (4)	0.944 (27)	1.17 (19)	0.9914 (22)	0.9997 (10)	1.0077 (24)	
HF/6-31 + G(d,p) (31)	1.011 (25)	0.944 (27)	1.17 (19)	0.9914 (22)	0.9997 (10)	1.0077 (24)	
HF/6-31 + G(3df,2p) (19)	1.000 (12)	0.944 (27)	1.17 (18)	0.9915 (19)	0.9997 (10)	1.0076 (21)	
HF/6-31 ++ G(d,p) (25)	1.008 (21)	0.950 (23)	1.17 (19)	0.9916 (18)	0.9998 (7)	1.0077 (24)	
HF/6-31 ++ G(3df,2p) (19)	0.999 (11)	0.944 (27)	1.17(19)	0.9915(19)	0.9997 (10)	1.0076 (21)	
HF/6-311G(d) (26)	0.977 (14)	0.941 (32)	1.19 (4)	0.991 (24)	0.9990 (33)	1.0088 (36)	
HF/cc-pVDZ (28)	0.973 (18)	0.952 (20)	1.19 (4)	0.989 (36)	0.9995 (18)	1.0086 (33)	
HF/aug-cc-pVDZ (22)	0.972 (20)	0.949 (24)	1.19 (4)	0.991 (24)	0.9994 (25)	1.0083 (30)	
HF/cc-pVTZ (26)	0.976 (16)	0.941 (32)	1.20 (1)	0.990 (30)	0.9993 (28)	1.0085 (31)	
Post-Hartree – Fock methods							
MP2/6-31G(d) (15)	0.971 (22)	0.968 (14)	1.20 (1)	0.991 (24)	0.9991 (30)	1.0074 (17)	
CASSCF(4,4)/6-31G(d) (24)	0.921 (35)	0.941 (32)	1.18 (14)	0.995 (5)	1.0022 (38)	1.0075 (18)	
MP2/6-31 + G(d,p) (3)	0.992 (1)	0.952 (20)	1.19 (4)	0.9929 (15)	1.0000 (1)	1.0068 (10)	
MC-QCISD/ML (4)	0.982 (8)	0.982 (9)	1.19 (4)	0.991 (24)	0.9994 (25)	1.0071 (6)	
MG3/ML (29)	1.011 (25)	0.946 (26)	1.17 (19)	0.991 (24)	0.9999 (4)	1.0075 (18)	
DFT methods							
B3LYP/6-31G(d) (11)	1.014 (29)	1.001 (2)	1.17 (19)	0.992 (17)	1.0002 (7)	1.0069 (3)	
B1LYP/6-31G(d) (10)	1.004 (17)	0.993 (6)	1.17 (19)	0.9915 (19)	0.9997 (10)	1.0069 (3)	
BPW91/6-31G(d) (32)	1.016 (30)	0.955 (17)	1.14 (39)	0.996 (3)	1.0015 (36)	1.0050 (37)	
mPW1PW91/6-31G(d) (8)	1.003 (15)	1.000 (3)	1.18 (14)	0.991 (24)	0.9995 (18)	1.0071 (6)	
PCM-UAHF/mPW1PW91/6-31G(d) (7)	0.986 (3)	0.974 (12)	1.19 (4)	0.990 (30)	0.9994 (25)	1.0071 (6)	15.5
B(M)LYP/6-31G(d) (16)	0.993 (2)	0.967 (15)	1.16 (36)	0.994 (6)	1.0006 (22)	1.0060 (28)	
mPW1PW91/6-31 + G(d,p) (17)	1.011 (25)	0.959 (16)	1.17 (19)	0.993 (7)	1.0006 (22)	1.0063 (23)	
MPW1 K/6-31 + G(d,p) (5)	0.995 (6)	0.952 (20)	1.18 (14)	1.000 (1)	0.9915 (39)	1.0067 (12)	
MPW1KK-SRP/6-31 + G(d,p) (13)	0.981 (10)	0.944 (27)	1.19 (4)	0.990 (30)	0.9996 (16)	1.0071 (6)	
B(M)LYP/6-311 ++ G(2d,2p) (32)	1.020 (31)	0.947 (25)	1.16 (36)	0.993 (7)	1.0006 (22)	1.0062 (27)	
B1LYP/aug-cc-pVDZ (2)	0.984 (7)	0.996 (4)	1.17 (19)	0.993 (7)	1.0002 (7)	1.0070 (1)	
B3LYP/aug-cc-pVDZ (1)	0.994 (4)	1.005 (1)	1.17 (19)	0.993 (7)	1.0003 (10)	1.0070 (1)	
C-PCM-UAHF/B3LYP/aug-cc-pVDZ (6)	0.982 (8)	0.984 (8)	1.17 (19)	0.993 (7)	1.0004 (16)	1.0067 (12)	22.1
PCM-UAHF/B3LYP/aug-cc-pVDZ (11)	0.973 (18)	0.978 (11)	1.17 (19)	0.993 (7)	1.0005 (18)	1.0066 (15)	22.8
B3LYP/aug-cc-pVTZ (8)	1.013 (28)	0.994 (5)	1.17 (19)	0.993 (7)	1.0001 (4)	1.0069 (3)	

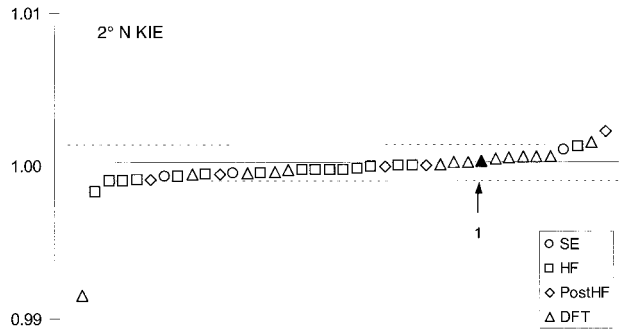

Figure 1. The nucleophile 2° nitrogen KIE calculated by the thirty-nine different theoretical methods for the ethyl chloride – cyanide ion S_N2 reaction. The horizontal lines on the Figure show the experimental average value ± two standard deviations. The arrow shows the value calculated by the B3LYP/aug-cc-pVDZ method (rank 1).

the PM3 with one explicit DMSO molecule (5.8 kcal mol^{-1}), and the SM5.4/PM3 (11.5 kcal mol^{-1}) methods.

Each theoretical method was ranked by its ability to calculate each KIE, Table 9. The ranking was established by using the absolute value of the difference between the calculated KIE and the median value of the experimental KIE. Then, the ranking for the ability to calculate all the KIEs was obtained by adding the rankings for each of the individual KIEs, excluding the nitrogen KIE, and this rank sum was used to determine the best overall method for calculating the experimental KIEs. The nitrogen KIE was excluded from this sum because most of the methods calculated this very small KIE very well, Figure 1, so large differences in the ranking did not mean that one method was less able to calculate this KIE than another. For example, the methods ranked 1 and 36 for

 © 2003 Wiley-VCH Verlag GmbH & Co. KGaA, Weinheim

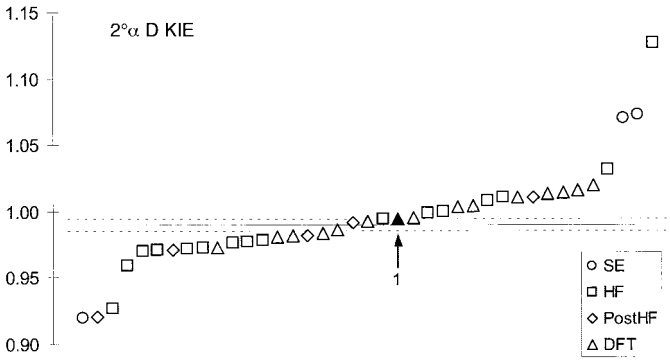

Figure 2. The 2° α-D KIE calculated by the thirty-nine different theoretical methods for the ethyl chloride – cyanide ion S_N2 reaction. The horizontal lines are the experimental minimum, median, and maximum values found for the KIE. The arrow shows the value calculated by the B3LYP/aug-cc-pVDZ method (rank 1).

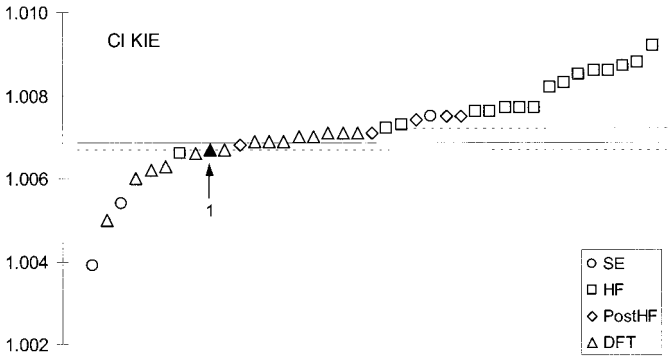

Figure 3. The chlorine leaving-group KIE calculated by the thirty-nine different theoretical methods for the ethyl chloride – cyanide ion S_N2 reaction. The horizontal lines are the experimental minimum, median, and maximum values found for the KIE. The arrow shows the value calculated by the B3LYP/aug-cc-pVDZ method (rank 1).

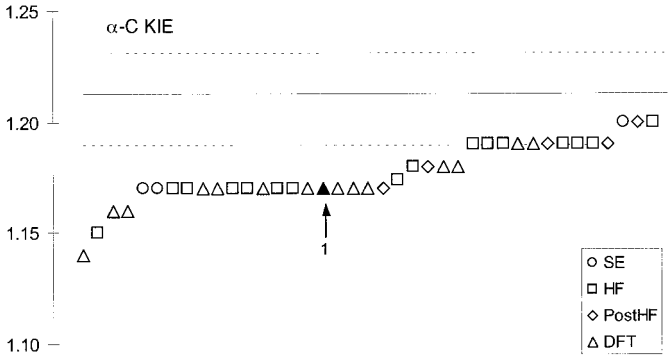

Figure 4. The α-carbon KIE calculated by the thirty-nine different theoretical methods for the ethyl chloride – cyanide ion S_N2 reaction. The horizontal lines are the experimental minimum, median, and maximum values found for the KIE. The arrow shows the value calculated by the B3LYP/aug-cc-pVDZ method (rank 1).

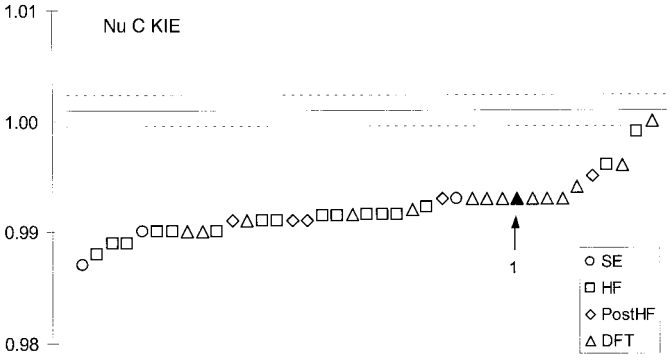

Figure 5. The nucleophile carbon KIE calculated by the thirty-nine different theoretical methods for the ethyl chloride – cyanide ion S_N2 reaction. The horizontal lines on the Figure show the experimental average value ± two standard deviations. The arrow shows the value calculated by the B3LYP/aug-cc-pVDZ method (rank 1).

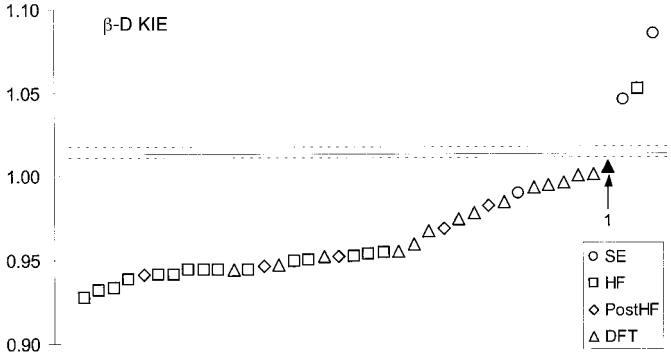

Figure 6. The 2° β-deuterium KIE calculated by the thirty-nine different theoretical methods for the ethyl chloride – cyanide ion S_N2 reaction. The horizontal lines are the experimental minimum, median, and maximum values found for the KIE. The arrow shows the value calculated by the B3LYP/aug-cc-pVDZ method (rank 1).

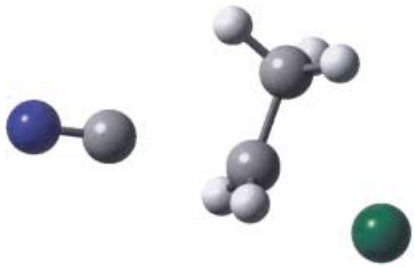

Figure 7. The transition-state structure calculated at the B3LYP/aug-cc-pVDZ level of theory for the S_N2 reaction between ethyl chloride and cyanide ion. The N≡C bond length is 1.177 Å, the C_N–C bond length is 2.341 Å, the C–Cl bond length is 2.291 Å, and the C_β–C bond length is 1.509 Å. The C_N-C-Cl bond angle is 164.2° and the Cl-C-C_β-H_β bond angle is 179.9°.

this KIE gave the experimental KIE and were equally good at calculating the KIE. An examination of the rankings in column 1 of Table 9, indicates that the two best methods were the density functional methods B3LYP/aug-cc-pVDZ and the B1LYP/aug-cc-pVDZ. The transition state calculated by using the B3LYP/aug-cc-pVDZ method is shown in Figure 7. It is also worth noting that even the best method only predicted two (the nucleophile 2° nitrogen and the 2° α-D KIEs) of the six experimental KIEs to within experimental error.

An inspection of the rankings in Table 9 reveals some interesting facts; correlated methods (post-Hartree – Fock and DFT) give the best results. A comparison of the calculations obtained by using the HF/6-31G basis set reveals that there is no trend in the quality of results when diffuse and polarization functions are used, although the system is negatively charged. This is in agreement with Jensen's findings.[86, 87] It is worth noting that the B3LYP functional

© 2003 Wiley-VCH Verlag GmbH & Co. KGaA, Weinheim

with the aug-cc-pVDZ basis set performed much better than the much more expensive MP2 and MC-QCISD methods. This list also shows a good performance by the mPW1PW91 functional, even in combination with a standard 6-31G(d) basis set. Among the DFT functionals, B3LYP, B1LYP, mPW1PW91, and MPW1K performed well, whereas BPW91 and B(M)LYP performed poorly. These findings are not surprising since BPW91 has problems with calculating the energetics correctly and B(M)LYP has been parameterized for weak hydrogen bonding, which is not present in the system studied. Finally, the poor performance of the semiempirical methods should be pointed out. Of these methods, AM1 is the best. It ranks average among all methods and substantially higher than other semiempirical methods. Finally, the inclusion of continuum solvent models (both PCM-UAHF and C-PCM-UAHF) do not significantly affect the results.

Solvent models: The methods of including solvent in quantum calculations are a subject of vigorous debate. A systematic study of solvation in KIE calculations for a model decarboxylation reaction[88] indicated the advantage of the continuum models over explicit inclusion of solvent molecules. Recent work from the Åquist group examined the ability of explicit solvent models to predict equilibrium oxygen isotope effects.[89] In the present study no systematic analysis of the solvation has been performed. Rather, a few readily available models were used, and the results were compared with those obtained in calculations at the same level of theory in the gas phase. In this part of the study the Onsager model, the COSMO model, the C-PCM-UAHF method, the PCM-UAHF method, and the SM5.4 and SM5.42 methods of considering solvent were applied at four theoretical levels, the HF/6-31G(d), the mPW1PW/6-31G(d), the B3LYP/aug-cc-pVDZ and the PM3 method. Only the SM5.42/HF/6-31G(d) method (which gave the exact value) and the COSMO/PM3 method gave values of the enthalpy of activation within four standard deviations of the experimental value.

In addition, a calculation with the inclusion of one explicit solvent molecule at the PM3 level was performed. The solvent molecule was positioned "behind" the nitrogen atom of the cyanide anion with the oxygen atom pointing at the nitrogen atom. The C_s symmetry of the starting model was not preserved in calculations, the Cl-C_α-C_β-$H_{\beta 1}$ torsional angle that should be 180° was 167.8° in the optimized structure. In the SM5.4/PM3 calculation the Cl-C_α-C_β-$H_{\beta 1}$ angle was found equal to 151.9° in the optimized structure. These results were therefore not considered.

The ranking of the methods in Table 9 shows that including the solvent does not have any significant effect on the results. This is undoubtedly due to the lack of sensitivity of these transition states (KIEs) to changes in solvent.[43–46] A detailed examination of the results in Table 9 shows that including the solvent only improves the results slightly in two out of the four tests. The gas-phase PM3 result that ranks 38th out of the 39 methods compared only moves up to 34th when the COSMO method is used in the calculation. The other improvement is that the mPW1PW91/6-31G(d) results move up from 8th to 7th position when combined with the PCM-UAHF solvent model. The results obtained at the HF/6-31G(d) level in the gas phase on the other hand, rank significantly lower upon inclusion of solvation, dropping from 13th position to 34th when the PCM-UAHF method is used, to 37th with COSMO, to 36th with SM5.42, and to 23rd when the Onsager model is used. Similar results were obtained for the DFT B3LYP/aug-cc-pVDZ method that yielded the best results among the methods studied. Here, including either the C-PCM-UAHF or the PCM-UAHF method lowered the ranking position from 1st to 6th or 11th, respectively. Thus, most of the gas-phase models perform better than the models that include a solvent environment for the cyanide ion – ethyl chloride S_N2 reaction. The two exceptions are the PM3/COSMO calculation, which leads to a small improvement, and the mPW1PW91/6-31G(d), which produced a marginally better result.

Conclusion

The six experimental KIEs measured for the S_N2 reaction between ethyl chloride and cyanide ion suggest that the transition state is late (product-like) with a short NC–C_α bond and a reasonably long C_α–Cl bond. All the theoretical methods, on the other hand, suggest that the transition state is very reactant-like and loose with little NC–C_α bond formation and significant C_α–Cl bond rupture. We have not been able to resolve the differences between the two approaches to determining transition-state structure for even this very simple reaction. One possibility is that all the theoretical methods fail to produce the correct transition structure. The fact that no method predicts all six KIEs correctly might indicate that this is, in fact, the case. Such a failure to yield correct transition structure could be due to theory's inability to calculate high-energy transition structures that are far from the ground state where theory works well and/or poor solvation modeling by the continuum models. The latter problem might be overcome by inclusion of a large number of explicit solvent molecules in the calculations. Another explanation is that the conventional framework for interpreting experimental KIEs may be flawed because it is based on empirical generalization and, at least partly, on approximate theory. A third alternative is that neither approach is able to predict the transition structure correctly. However, regardless of which is correct, the experimental KIEs presented provide a benchmark against which theoretical methods may be rigorously assessed. It is relatively easy to find a theoretical method that can be used to predict one or even two KIEs for a reacting system correctly. A more critical test, however, is whether a larger set of KIEs, such as for the six KIE in our study, may be predicted.

Although none of the theoretical methods was able to predict all six of the KIEs, the DFT methods were best able to generate the experimental KIEs. The two DFT methods, the B3LYP/aug-cc-pVDZ and the B1LYP/aug-cc-pVDZ were judged the best. Including solvation in the calculation did not significantly improve the fit to the experimental KIEs.

In terms of calculating the experimental KIEs, the best results were obtained for the very small secondary nitrogen KIE. This was undoubtedly found because there is little or no

 © 2003 Wiley-VCH Verlag GmbH & Co. KGaA, Weinheim

change in bonding to the cyanide ion nitrogen on going to the transition state. The second-best results were obtained for the 2° α-D followed by the chlorine KIEs. The α-carbon KIEs were calculated with less success. The theoretical methods were not successful in calculating the nucleophile carbon and the 2° β-D KIEs. In fact, hardly any of the methods were able to reproduce the last two experimental isotope effects. In this regard, it is worth noting that the calculated transition-state structures and force constants lead to a more inverse incoming-carbon KIE than is found experimentally. This suggests the theoretical methods may have difficulty calculating the vibrational energies involving the nucleophile–α-carbon bond in the S_N2 transition state. Two solvent models were able to reproduce the experimental activation energy.

Finally, although none of the theoretical methods used in this study was able to reproduce all of the experimental KIEs correctly, theoretical calculations of KIEs are an important tool in physical organic chemistry. For instance, KIEs calculated by theoretical methods are often sufficiently accurate to distinguish between possible mechanistic alternatives and several papers by Houk,[90, 91] Schramm,[92, 93] and Truhlar[94, 95] are good examples of the usefulness of theoretical methods for determining reaction mechanisms. Using theoretical methods to investigate special attributes of a reaction within a specific system is also believed to be very useful. For example, the theoretical experiments of ion pairing and negative-ion hyperconjugation in elimination reactions by Saunders,[96–98] the studies of E2 elimination and S_N2 reactions by Glad and Jensen[86, 87] and the studies of S_N2 reactions by Williams and co-workers[99–101] and by Westaway and co-workers[11] are important investigations of specific effects that have led to important additions to the theory of kinetic isotope effects and the factors that affect their magnitude.

Experimental Section

Preparation of Materials: Tetrabutylammonium cyanide (97%, Aldrich), chloroethane (98%, Ferak Berlin, Germany), dimethylsulfoxide (99.5%, Fluka or Caledon Laboratories, anhydrous, distilled in glass grade), and nickel(II) nitrate hexahydrate (99%, POCh Gliwice, Poland) were used without further purification. The tetrabutylammonium cyanide was kept in a vacuum desiccator once it had been opened.

Ethyl chloride: Ethanol (20 mL, ca. 15.8 g, 0.343 mol) was added slowly to a cold mixture of anhydrous zinc chloride (92 g) and concentrated hydrochloric acid (58 mL) in a 100 mL three-necked round-bottom flask. The flask was cooled in an ice–salt bath so that the temperature remained below 8 °C to prevent any loss of hydrogen chloride during the addition to the zinc chloride. The flask was fitted with a vertical water-cooled five-bulb reflux condenser attached to a set of four gas traps. The first two gas traps contained water for absorbing hydrogen chloride and the last two contained concentrated sulfuric acid for adsorbing any water from the first gas traps. A vented test tube immersed in an ice–salt bath was connected to the final gas trap to collect the ethyl chloride. A slow stream of nitrogen was applied through one neck of the three-necked reaction flask to provide a positive pressure in the system. A thermometer was inserted in the third neck of the flask to measure the temperature of the reaction mixture.

The reaction mixture was heated slowly to 105 °C, and the ethyl chloride was distilled. The temperature of the reaction mixture was gradually raised to 130 °C to increase the yield of ethyl chloride. All the ethyl chloride was collected between 30 and 45 minutes after the reaction mixture began to boil. The yield of ethyl chloride was 16 mL (ca. 14.4 g, 65%). An NMR spectrum was consistent with that for ethyl chloride.

(1,1-$^2H_2$)Ethyl chloride: (1,1-$^2H_2$)ethanol (10 g, 0.208 mol, Sigma–Aldrich, 98 atom% D_2) was treated with a mixture of zinc chloride (56 g) in concentrated hydrochloric acid (35 mL) by using the procedure described above. The yield of (1,1-$^2H_2$)ethyl chloride was 3 mL (2.7 g, 20%). An NMR spectrum indicated that the product was 99.0% deuterated at the 1-position.

(2,2,2-$^2H_3$)Ethyl chloride: (2,2,2-$^2H_3$)ethanol (10 g, 0.204 mol, Sigma–Aldrich, 99 atom% D_3) was treated with a mixture of zinc chloride (56 g) in concentrated hydrochloric acid (35 mL) by using the procedure described for the synthesis of ethyl chloride. The yield of (2,2,2-$^2H_3$)ethyl chloride was 3 mL (2.7 g, 21%). An NMR spectrum indicated that the product was 99.2% deuterated at the 2-position.

[1-^{11}C]Ethyl chloride: [1-^{11}C]Ethanol[102] (1–2 GBq) dissolved in concentrated hydrochloric acid (0.4 mL) was added with a syringe to a septum-covered 3 mL conical glass vial containing anhydrous $ZnCl_2$ (0.7 g). The mixture was heated to 130 °C for 4 min, and then the [1-^{11}C]ethyl chloride was distilled by bubbling a slow stream of nitrogen (10 mL min^{-1}) through the solution. The gas stream was passed through an aqueous solution of NaOH (4 mL, 1M) and then through a drying tower containing sicapent. Finally, the [1-^{11}C]ethyl chloride was trapped in DMSO (0.5 mL) at 20 °C. The amount of trapped radioactivity reached its maximum after 3 min. Typically 200–300 MBq of [1-^{11}C]ethyl chloride was obtained.

[1-^{14}C]Ethyl chloride: [1-^{14}C]Ethanol (10 MBq, American Radiolabeled Chemicals Inc.) dissolved in concentrated hydrochloric acid (0.4 mL) was added with a syringe to a septum-covered 3 mL conical glass vial containing anhydrous $ZnCl_2$ (0.7 g). The mixture was then heated to 130 °C under a slow stream of nitrogen (10 mL min^{-1}). The gas stream was passed through an aqueous solution of NaOH (4 mL, 1M) and then through a drying tower containing siccapent. Finally, the [1-^{14}C]ethyl chloride was trapped in THF (1 mL) at −40 °C. About 6 MBq of product was obtained.

Determination of the secondary α- and β-deuterium KIEs: A solution of the cyanide ion (0.25M) was prepared by dissolving tetrabutylammonium cyanide (1 g) in anhydrous, distilled-in-glass grade DMSO (15 mL, Caledon Laboratories) under a nitrogen atmosphere in an I^2R glove bag. A ethyl chloride stock solution (0.12M) was prepared by injecting ethyl chloride or deuterated ethyl chloride (400 μL) from a 500 μL syringe that had been cooled in a deep freeze and kept in the freezer wrapped in plastic bags to avoid condensation of water, into a sample vial containing anhydrous DMSO (15 mL) and sealed with a rubber septum. The free space above the solvent in the vial was kept to less than 1 mL to reduce the risk of evaporation of the ethyl chloride. The amount of ethyl chloride added to the vial was determined by precisely measuring the weights of the vial before and after the ethyl chloride was added.

Both stock solutions were placed in a constant-temperature bath at 30.000 ± 0.002 °C for 1 h. Then, the reaction was started by injecting the ethyl chloride stock solution (5 mL) into the tetrabutylammonium cyanide solution so that the final concentrations were 0.030 and 0.188M for the ethyl chloride and the tetrabutylammonium cyanide, respectively. Aliquots (1 mL) of the reaction mixture were taken at various times throughout the reaction and injected into nitric acid (30 mL 0.013M); this quenched the reaction by converting the unreacted cyanide ion into HCN.

The acidic solution was stirred in the fume hood for at least an hour to completely remove the hydrogen cyanide.

Finally, the chloride ion in the sample was analyzed in a potentiometric titration by using a standard silver nitrate solution (0.005M).[103]

The KIE was determined by dividing the rate constants measured separately for the deuterated and undeuterated isotopomers.

Determination of the chlorine KIE: The chlorine KIE was measured by carrying out the reaction in the same way as the secondary α- and β-deuterium KIEs were measured. The reactions were quenched at extents of reaction varying from 11 to 22% completion by pouring the whole reaction mixture into nitric acid (30 mL, 0.013M). After the hydrogen cyanide had been removed (vide supra), the samples were titrated with standard silver nitrate (0.005M) in a potentiometric titration,[103] and the silver chloride precipitate was filtered and converted into methyl chloride by using the

© 2003 Wiley-VCH Verlag GmbH & Co. KGaA, Weinheim

standard procedure.[104] The chlorine KIE was determined from Equation (4):

$$k^{35}/k^{37} = \frac{\ln(1-f)}{\ln[1-(R_o/R_f)f]} \quad (4)$$

in which R_o and R_f are the ratios of the chlorine isotopes in the reactant before reaction and in the product (chloride ion) after a fraction of reaction f, respectively. The $^{37}Cl/^{35}Cl$ ratios, R_i ($i = 0, f$), were calculated from the $\delta^{37}Cl$ values obtained from the isotope-ratio mass spectrometric measurements[105] by using Equation (5):

$$R_i = R_{ST}\,(1 + \delta_i/1000) \quad (5)$$

here R_{ST} is the $^{37}Cl/^{35}Cl$ ratio found for a standard methyl chloride sample. The R_o value was obtained by analyzing the chloride ion from the S_N2 reaction between ethyl chloride and sodium thiophenoxide in DMSO at 20 °C, a reaction found to go to 100 % completion. This was necessary because the cyanide ion – ethyl chloride reaction in DMSO could not be taken to 100 % completion, presumably because some of the volatile ethyl chloride was lost before the slow cyanide-ion reaction reached 100 % completion. Using this faster reaction at a lower temperature for determining the R_o value corrected the error associated with the failure to get the ethyl chloride – cyanide ion reaction to go to 100 % completion.

Determination of the nucleophile carbon and nitrogen KIEs: The carbon and nitrogen nucleophile kinetic isotope effects were measured by using the "dead-end" conditions for the kinetic runs; that is, a molar excess of tetrabutylammonium cyanide with respect to the ethyl chloride was used for each experiment so that a predefined fraction of the cyanide ion had reacted when all the ethyl chloride had been consumed. Since ethyl chloride is very volatile, the volume of the solution was chosen so that the space between the stopper and the surface of the solution was negligible. These technical constraints caused a slight variation in the concentrations of the reactants in each run, that is, the ethyl chloride (98 %; Ferak Berlin, Germany) varied from 0.03 to 0.08 M and the tetrabutylammonium cyanide varied from 0.09 to 0.17 M in DMSO. The reaction mixtures were shaken at 30 °C for 7 h to ensure that the reaction had gone to completion. Then, nickel nitrate (300 mg) was added to each sample to precipitate the unreacted cyanide ion. The solution was separated in a centrifuge, the solvent was decanted, and the residue was washed with water. This procedure was repeated three times to remove all the nitrate ion and other reactants. Then, the nickel cyanide was dried in a desiccator over molecular sieves. Approximately 10 mg of the nickel cyanide was used for determining the isotopic ratio of the carbon and nitrogen atoms by isotope-ratio mass spectrometry on a Finnigan Delta S mass spectrometer combined in-line with a Heraeus elemental analyzer. Nickel cyanide was also used to determine the isotopic composition of the carbon and nitrogen atoms in the initial cyanide ion. Although the fraction of reaction, f, was calculated from the concentration of the reactants, the actual fraction of reaction was confirmed by using a standard colorimetric assay for the chloride ion.[105] The two methods agreed within ±0.1 %. The isotope effect k^{14}/k^{15}, was determined from the isotopic composition of the reactant remaining after fraction of reaction f from the slope of the linear dependence of $\ln(1000 + \delta_f)$ on $\ln(1-f)$:

$$\ln(1000 + \delta_f) = \left(\frac{1}{k^{14}/k^{15}} - 1\right)\ln(1-f) + \ln(1000 + \delta_0) \quad (6)$$

Determination of the $^{11}C/^{14}C$ α-Carbon KIE: [1-^{14}C]ethyl chloride (30 MBq) in THF (5 μL,) was added to a solution of [1-^{11}C]ethyl chloride (100 – 300 MBq) in DMSO (0.5 mL). After careful mixing, a 30 μL sample was injected into the HPLC and the reactant fraction $t_r = 15.4 - 16.5$ min was collected. The HPLC separation was performed on a Phenomenex spherisorb 5 ODS(2) 250 × 4.6 mm ID C_{18} column with a Beckman 126 gradient pump in series with a β^+ flow detector. The mobile phases were acetonitrile (A) and ammonium formate (0.05 M) at pH 3.5 (B). The gradient used was from 0 to 6 min: 10 % A, from 6 to 7 min: the composition changed from 10 to 35 % A, 7 – 16 min: 35 – 50 % A, 16 – 17 min: 50 – 95 % A, and 21 – 22 min: 95 – 100 % A. The flow rate was 1 mL min^{-1}. Data collection and HPLC control were performed with a Beckman System Gold chromatograph software package. Sample injection and fraction collection were performed on a Gilson 231 XL sampling injector that was coupled to a Gilson 401 C dilutor.

Then, the rest of the DMSO solution was transferred to a capped vial containing tetrabutylammonium cyanide (70 mg) and the vial was shaken to dissolve the latter. The vial was kept at 30 °C in the thermostated sample rack of the HPLC. At 30 min intervals, 30 μL aliquots were injected into the HPLC, and the reactant (ethyl chloride) fractions were collected in scintillation vials containing scintillation liquid. A dummy fraction was collected just before the reactant fraction to rinse the fraction collector and to prevent contamination from any radioactivity remaining from a previous fraction. The total radioactivity (^{11}C + ^{14}C) in the collected reactant fractions was measured by liquid scintillation counting with a counting time of 3 – 5 min per sample. The liquid scintillation counting was performed with a Beckman LS 6000 LL liquid scintillation counter in the wide-open mode by using Zinsser Quicksafe A as the scintillation cocktail in Zinsser 20 mL poly vials.

The amount of radioactivity in the samples varied between 50 000 and 300 000 counts per minute. When all of the ^{11}C radioactivity had decayed, usually the next day, the samples were remeasured to give the ^{14}C radioactivity. The ^{14}C data were corrected for ^{14}C background by analyzing the reactant fraction for ^{14}C radioactivity when the reaction had gone to completion. The ^{14}C radioactivity was subtracted from the total radioactivity to give the ^{11}C radioactivity. The ^{11}C radioactivity was then corrected for decay and the $^{14}C/^{11}C$ isotopic ratios, R_f and R_0 at the different reaction points, were calculated. The point KIEs, k^{11}/k^{14}, were calculated by using Equation (7):

$$\frac{k^{11}}{k^{14}} = \frac{\ln(1-f)}{\ln[(1-f)R_f/R_0]} \quad (7)$$

The fractional conversion f for each point was calculated from the integrated radio detector peaks of the ^{11}C reactant and product, after correcting the peak areas for decay due to different retention times.

Acknowledgement

The authors wish to express their thanks to the Natural Sciences and Engineering Research Council of Canada (NSERC), the State Committee for Scientific Research (KBN, Poland), the Joint Maria Skłodowska-Curie Polish – American Funds II, NATO, and the Swedish Science Research Council (NFR/VR). The authors also wish to thank Professor Bengt Långström for providing general radiochemical support and for allowing us to use the excellent facilities at the Uppsala University PET Centre. Computing resources were provided by national computing facilities at Warsaw, Krakow, and Poznan, Poland.

[1] R. F. Hudson, G. Klopman, *J. Chem. Soc.* **1962**, 1062.
[2] F. P. Ballistreri, E. Maccarone, A. Mamo, *J. Org. Chem.* **1976**, 41, 3364.
[3] K. M. Koshy, R. E. Robertson, *J. Am. Chem. Soc.* **1974**, 96, 914.
[4] K. C. Westaway, Z. Waszczylo, *Can. J. Chem.* **1982**, 60, 2500.
[5] M. P. Friedberger, E. R. Thornton, *J. Am. Chem. Soc.* **1976**, 98, 2861.
[6] V. J. Shiner, Jr., F. P. Wilgis in *Isotopes in Organic Chemistry*, *Vol. 8* (Eds.: E. Buncel, W. H. Saunders, Jr.) Elsevier, Amsterdam, **1992**, pp. 245 – 246.
[7] S. F. Ali, K. C. Westaway, *Can. J. Chem.* **1979**, 57, 1354.
[8] O. Matsson, J. Persson, B. S. Axelsson, B. Långström, Y. Fang, K. C. Westaway, *J. Am. Chem. Soc.* **1996**, 118, 6350.
[9] K. C. Westaway, Y.-r. Fang, J. Persson, O. Matsson, *J. Am. Chem. Soc.* **1998**, 120, 3340.
[10] See for example, J. P. Klinman in *Enzyme Mechanism from Isotope Effects* (Ed.: P. F. Cook), CRC Press, Boca Raton, **1991**, Chapter 4, and references therein.
[11] R. A. Poirier, Y. Wang, K. C. Westaway, *J. Am. Chem. Soc.* **1994**, 116, 2526.
[12] K. C. Westaway, T. V. Pham, Y.-r. Fang, *J. Am. Chem. Soc.* **1997**, 119, 3670.
[13] B. S. Axelsson, O. Matsson, B. Långström, *J. Am. Chem. Soc.* **1990**, 112, 6661.

 © 2003 Wiley-VCH Verlag GmbH & Co. KGaA, Weinheim

[14] C. H. Gray, J. K. Coward, K. B. Schowen, R. L. Schowen, *J. Am. Chem. Soc*. **1979**, *101*, 4351.
[15] L. B. Sims, D. E. Lewis in *Isotopes in Organic Chemistry*, *Vol. 6* (Eds.: E. Buncel, C. C. Lee), Elsevier, Amsterdam, **1984**.
[16] J. Rodgers, D. A. Femec, R. L. Schowen, *J. Am. Chem. Soc*. **1982**, 104, 3263.
[17] R. Fuchs, J. L. Bear, R. F. Rodewald, *J. Am. Chem. Soc*. **1969**, 91, 5797.
[18] J. I. Padova in *Modern Aspects of Electrochemistry*, *Vol. 7* (Eds. E. B. Conway, J. O'M. Bockris), Butterworths, London, **1971**, pp. 8–21.
[19] D. K. Bohme, G. I. Mackay, *J. Am. Chem. Soc*. **1981**, 103, 978.
[20] M. J. Pellerite, J. I. Brauman, *J. Am. Chem. Soc*. **1980**, 102, 5993.
[21] S. Wolfe, D. J. Mitchell, H. B. Schlegel, *J. Am. Chem. Soc*. **1981**, 103, 7694.
[22] K. C. Westaway in *Isotopes in Organic Chemistry*, Vol. 7 (Eds.: E. Buncel, C. C. Lee), Elsevier, Amsterdam, **1987**, Chapter 5.
[23] The following labeling is used throughout the paper in order to distinguish atoms of the same element in different positions: C_α–central (methylene) carbon, C_β–methyl carbon, H_α–methylene hydrogens, H_β–methyl hydrogens, $H_{\beta 1}$–methyl hydrogen atom in a *trans* position to the chlorine atom.
[24] V. J. Shiner, Jr. in *Isotope Effects in Chemical Reactions* (Eds.: C. J. Collins, N. S. Bowman), A.C.S. Publication 167, Van Nostrand–Reinhold, New York, **1970**, pp. 90–135.
[25] K. C. Westaway, Z.-g. Lai, *Can. J. Chem*, **1989**, 67, 345.
[26] K. C. Westaway, abstracts of papers, International Isotope Society Symposium on Isotope Separation and Applications, Ottawa, **1998**, Abstract.
[27] J. W. Hill, A. Fry, *J. Am. Chem. Soc*. **1962**, 84, 2763.
[28] T. Koerner, Y.-r. Fang, K. C. Westaway, *J. Am. Chem. Soc*. **2000**, 122, 7342.
[29] J. V. Shiner, Jr. in *Isotope Effects in Chemical Reactions* (Eds.: J. C. Collins, S. N. Bowman), A.C.S. Publication 167, Van Nostrand–Reinhold, New York, **1970**, p. 144.
[30] K. C. Westaway in *Isotopes in Organic Chemistry*, *Vol. 7* (Eds. E. Buncel, C. C. Lee), Elsevier, Amsterdam, **1987**, pp. 287, 305–306.
[31] A. Maccoll in *The Chemical Soc. Annual Reports A*, **1974**, 71, 77.
[32] E. W. Buddenbaum, J. V. Shiner, Jr. in *Isotope Effects on Enzyme Catalyzed Reactions* (Eds. W. W. Cleland, H. M. O'Leary, B. D. Northrop), University Park Press, London, **1977**, p. 18.
[33] K. R. Lynn, P. E. Yankwich, *J. Am. Chem. Soc*. **1961**, *83*, 3220.
[34] J. Bigeleisen, *J. Phys. Chem*. **1952**, *56*, 823.
[35] M. J. Stern, P. C. Vogel, *J. Chem. Phys*. **1971**, *55*, 2007.
[36] K. R. Lynn, P. E. Yankwich, *J. Am. Chem. Soc*. **1961**, *83*, 790.
[37] B. S. Axelsson, O. Matsson, B. Långström, *J. Phys. Org. Chem.* **1991**, *4*, 77.
[38] J. Persson, U. Berg, O. Matsson, *J. Org. Chem.* **1995**, *60*, 5037.
[39] H. Yamataka, T. Ando, *J. Phys. Chem.* **1981** , *85*, 2281.
[40] The magnitude of the KIE is related to the change in the bond order, not to the geometry, i.e., the bond lengths, in the transition state. However, the [(length of the transition state bond – length of the stable bond in the reactant or product)/length of the normal bond in the reactant or product] $\times 100\,\%$ is related to the change in bond order on going to the transition state.[21]
[41] Calculations suggest that the nucleophile–alpha carbon bond would have to be ≤ 1.5 times the length of the normal carbon–carbon bond before the magnitude of the incoming carbon KIE is affected.
[42] A. González-Lafont, J. Villá, J. M. Lluch, J. Bertrán, R. Steckler, D. G. Truhlar, *J. Phys. Chem. A*. **1998**, *102*, 3420, and references 11–18 therein.
[43] K. C. Westaway, *Can. J. Chem*. **1978**, *56*, 2691.
[44] D. G. Graczyk, W. J. Taylor, R. C. Turnquist, *J. Am. Chem. Soc*. **1978**, *100*, 7333.
[45] K. C. Westaway, Z.-g. Lai, *Can. Chem. J.* **1989**, 67, 345.
[46] K. C. Westaway, Y. Gao, Y.-r. Fang, *J. Org. Chem.* **2003**, in press.
[47] M. J. S. Dewar, E. G. Zoebisch, E. F. Healy, J. J. P. Stewart, *J. Am. Chem. Soc.* **1985**, *107*, 3902.
[48] J. J. P. Stewart, *J. Comp. Chem*. **1989**, *10*, 209; J. J. P. Stewart, *J. Comp. Chem.* **1989**, *10*, 221.
[49] M. J. S. Dewar, C. Jie, G. Yu, *Tetrahedron*, **1993**, *23*, 5003.
[50] J. A. Holder, R. D. Dennington, C. Jie, G. Yu, *Tetrahedron*, **1994**, *50*, 627.
[51] R. E. Easton, D. J. Giesen, A. Welch, C. J. Cramer, D. G. Truhlar, *Theor. Chim. Acta* **1996**, *93*, 281.
[52] B. J. Lynch, P. L. Fast, M. Harris, D. G. Truhlar, *J. Phys. Chem. A* **2000**, *104*, 4811.
[53] T. H. Dunning, Jr., P. J. Hay in *Modern Theoretical Chemistry, Vol. 3*, (Ed.: H. F. Schaefer III), Plenum, New York, **1976**, p. 1.
[54] D. E. Woon, T. H. Dunning, Jr., *J. Chem. Phys.* **1993**, *98*, 1358.
[55] R. A. Kendall, T. H. Dunning, Jr., R. J. Harrison, *J. Chem. Phys.* **1992**, *96*, 6796.
[56] P. C. Hariharan, J. A. Pople, *Theor. Chim. Acta* **1973**, *28*, 213.
[57] M. J. S. Dewar, C. H. Reynolds, *J. Comp. Chem*. **1986**, *2*, 140.
[58] A. D. McLean, G. S. Chandler, *J. Chem. Phys*. **1980**, *72*, 5639.
[59] T. Clark, J. Chandrasekhar, G. W. Spitznagel, P. v. R. Schleyer, *J. Comp. Chem*. **1983**, *4*, 294.
[60] M. J. Frisch, J. A. Pople, J. S. Binkley, *J. Chem. Phys*. **1984**, *80*, 3265.
[61] A. D. Becke, *Rev. Phys. A* **1988**, *38*, 3098.
[62] A. D. Becke, *J. Chem. Phys*. **1993**, *98*, 5648.
[63] A. D. Becke, *J. Chem. Phys*. **1996**, *104*, 1040.
[64] C. Adamo, V. Barone, *J. Chem. Phys*. **1998**, *108*, 664.
[65] J. Lundell, Z. Latajka, *J. Phys. Chem. A* **1997**, *101*, 5004.
[66] J. P. Perdew, J. A. Chevary, S. H. Vosko, K. A. Jackson, M. R. Pederson, D. J. Singh, C. Fiolhais, *Phys. Rev. B* **1992**, 46.
[67] C. Lee, W. Yang, G. Parr, *Rev. Phys. A* **1988**, *37*, 785.
[68] B. J. Lynch, P. L. Fast, M. Harris, D. G. Truhlar, *J. Phys. Chem. A* **2000**, *104*, 4811.
[69] A. Gonzalez-Lafont, T. N. Truong, D. G. Truhlar, *J. Phys. Chem.* **1991**, *95*, 4618.
[70] C. Möller, M. S. Plesset, *Phys. Rev.* **1934**, *46*, 618.
[71] P. L. Fast, M. L. Sanchez, D. G. Truhlar, *Chem. Phys. Lett.* **1999**, *306*, 407.
[72] P. L. Fast, D. G. Truhlar, *J. Phys. Chem. A.* **2000**, *104*, 6111.
[73] D. Hegarty, M. A. Robb, *Mol. Phys*. **1979**, *38*, 1795.
[74] A. Klamt, G. J. Schüürmann, *J. Chem. Soc. Perkin Trans. 2*. **1993**, 799.
[75] a) D. J. Giesen, C. C. Chambers, C. J. Cramer, D. G. Truhlar, *J. Phys. Chem.* **1997**, *101*, 2061; b) D. J. Giesen, G. D. Hawkins, D. A. Liotard, C. J. Cramer, D. G. Truhlar, *Theor. Chem. Acc.* **1997**, *98*, 85.
[76] a) T. Zhu, J. Li, D. A. Liotard, C. J. Cramer, *J. Chem. Phys.* **1999**, *110*, 5503; Y.-Y. Chuang, M. L. Radhakrishnan, P. L. Fast, C. J. Cramer, D. G. Truhlar, *J. Phys. Chem. A.* **1999**, *103*, 4893; b) J. Li, G. D. Hawkins, C. J. Cramer, D. G. Truhlar, *Chem. Phys. Lett.* **1998**, *288*, 293; c) J. Li, T. Zhu, G. D. Hawkins, P. Winget, D. A. Liotard, C. J. Cramer, D. G. Truhlar, *Theor. Chem. Acc.* **1999**, *103*, 9.
[77] V. Barone, M. Cossi, *J. Phys. Chem. A.* **1998**, *102*, 1995.
[78] S. Miertus, E. Scrocco, J. Tomasi, *Chem. Phys*. **1981**, *55*, 117.
[79] a) L. Onsager, *J. Am. Chem. Soc*. **1936**, *58*, 1486; b) M. W. Wong, M. J. Frisch, K. B. Wiberg, *J. Am. Chem. Soc*. **1991**, *113*, 4776.
[80] G. D. Hawkins, D. J. Giesen, G. C. Lynch, C. C. Chambers, J. Rossi, J. W. Storer, J. Li, D. Rinaldi, D. A. Liotard, C. J. Cramer, D. G. Truhlar, AMSOL-version 6.5.1, **1998**.
[81] FQS Poland (Fujitsu), **2001**.
[82] J. M. Rodgers, B. J. Lynch, P. L. Fast, Y.-Y. Chuang, J. Pu, G. D. Truhlar, MULTILEVEL-version 2.3/G98, University of Minnesota, Minneapolis, **2001**.
[83] Gaussian 98 (Revision A.9), M. J. Frisch, G. W. Trucks, H. B. Schlegel, G. E. Scuseria, M. A. Robb, J. R. Cheeseman, V. G. Zakrzewski, J. A. Montgomery, R. E. Stratmann, J. C. Burant, S. Dapprich, J. M. Millam, A. D. Daniels, K. N. Kudin, M. C. Strain, O. Farkas, J. Tomasi, V. Barone, M. Cossi, R. Cammi, B. Mennucci, C. Pomelli, C. Adamo, S. Clifford, J. Ochterski, G. A. Petersson, P. Y. Ayala, Q. Cui, K. Morokuma, D. K. Malick, A. D. Rabuck, K. Raghavachari, J. B. Foresman, J. Cioslowski, J. V. Ortiz, B. B. Stefanov, G. Liu, A. Liashenko, P. Piskorz, I. Komaromi, R. Gomperts, R. L. Martin, D. J. Fox, T. Keith, M. A. Al-Laham, C. Y. Peng, A. Nanayakkara, C. Gonzalez, M. Challacombe, P. M. W. Gill, B. G. Johnson, W. Chen, M. W. Wong, J. L. Andres, M. Head-Gordon, E. S. Replogle, J. A. Pople, Gaussian, Inc., Pittsburgh, PA, **1998**.
[84] V. Anisimov, P. Paneth, *J. Math. Chem*. **1999**, *26*, 75.
[85] M. P. Meyer, A. J. DelMonte, D. A. Singleton, *J. Am. Chem. Soc.* **1999**, *121*, 10865.
[86] a) S. S. Glad, F. Jensen, *J. Am. Chem. Soc*. **1994**, 116, 9302; b) S. S. Glad, F. Jensen, *J. Org. Chem*. **1997**, 62, 253.

© 2003 Wiley-VCH Verlag GmbH & Co. KGaA, Weinheim

[87] S. S. Glad, F. Jensen, *J. Am. Chem. Soc.* **1997**, 119, 227.
[88] a) D. Sicinska, D. G. Truhlar, P. Paneth, *J. Am. Chem. Soc.* **2001**, *123*, 7683; b) D. Sicinska, P. Paneth, D. G. Truhlar, *J. Phys. Chem. B* **2002**, *106*, 2708.
[89] K. Kolmodin, V. B. Luzhkov, J. Åqvist, *J. Am. Chem. Soc.* **2002**, *124*, 10130.
[90] A. E. Keating, S. R. Merrigan, D. A. Singleton, K. N. Houk, *J. Am. Chem. Soc.* **1999**, *121*, 3933.
[91] a) B. R. Beno, K. N. Houk, D. A. Singleton, *J. Am. Chem. Soc.* **1996**, *118*, 9984; b) A. J. DelMonte, J. Haller, K. N. Houk, K. B. Sharpless, D. A. Singleton, T. Strassner, A. A. Thomas, *J. Am. Chem. Soc.* **1997**, *119*, 9907.
[92] P. J. Berti, V. L. Schramm, *J. Am. Chem. Soc.* **1997**, *119*, 12069.
[93] a) P. C. Kline, V. L. Schramm, *Biochemistry*, **1993**, *32*, 13212; b) P. C. Kline, V. L. Schramm, *Biochemistry*, **1995**, *34*, 1153.
[94] a) A. A. Viggiano, J. Paschkewitz, R. A. Morris, J. F. Paulson, A. Gonzales-Lafont, D. G. Truhlar, *J. Am. Chem. Soc.* **1991**, *113*, 9404; b) W.-P. Hu, D. G. Truhlar, *J. Am. Chem. Soc.* **1995**, *117*, 10726.
[95] V. S. Melissas, D. G. Truhlar, *J. Chem. Phys.* **1993**, *99*, 3542.
[96] W. H. Saunders, Jr., *J. Org. Chem.* **2000**, *65*, 681.
[97] W. H. Saunders, Jr., *J. Org. Chem.* **1997**, *62*, 244.
[98] W. H. Saunders, Jr., *J. Org. Chem.* **1999**, *64*, 861.
[99] G. D. Ruggiero, I. H. Williams, *J. Chem. Soc. Perkin Trans. 2*, **2002**, 591.
[100] G. D. Ruggiero, I. H. Williams, *J. Chem. Soc. Perkin Trans. 2*, **2001**, 448.
[101] V. Moliner, I. H. Williams, *J. Am. Chem. Soc.* **2000**, *122*, 10895.
[102] The [1-^{11}C]ethanol was produced at the Uppsala PET-Centre by a procedure that will be published elsewhere by J. Eriksson and B. Långström.
[103] K. C. Westaway, Z.-g. Lai, *Can. J. Chem*, **1988**, *66*, 1263.
[104] K. C. Westaway, T. Koerner, Y.-r. Fang, J. Rudzinski, P. Paneth, *Anal. Chem*. **1998**, *70*, 3548.
[105] I. Iwasaki, S. Utsumi, K. Hagino, T. Ozawa, *Bull. Chem. Soc. Jpn*. **1956**, *29*, 860.

Received: May 23, 2002
Revised: January 14, 2003 [F4119]

 © 2003 Wiley-VCH Verlag GmbH & Co. KGaA, Weinheim